# Capacitance-transient-spectroscopy model for defects with two charge states

E. F. Ferrari,* M. Koehler, and I. A. Hümmelgen
*Departamento de Física, Universidade Federal do Paraná, Caixa Postal 19081, 81531-990 Curitiba Paraná, Brazil*
(Received 13 March 1996; revised manuscript received 21 October 1996)

We formulate the set of coupled differential equations that govern the charge capture and emission process of deep levels that present two possible charge states. This solution is obtained considering the steady-state conditions imposed by DLTS (deep level transient spectroscopy) technique procedure. We distinguish three types of defects according to the predominance of one of the three different emission processes. Using our model, we reproduce DLTS spectra of doubly charged defects observed in different semiconductors such as *p*-type CdTe, electron and proton irradiated *n*-type GaAs, and sulfur-doped GaSb. Thermal barriers for carrier capture are easily introduced in our equations permitting one to reproduce experimental data even in the case of large lattice relaxation. We show that without a further analysis within the framework of our model, some DLTS spectra of defects with two states of charge might be misinterpreted as is the case for the *DX* center in GaSb:S. [S0163-1829(97)01615-9]

## I. INTRODUCTION

The presence of deep levels can strongly influence the charge carrier transport and lifetime in semiconductors. For this reason several techniques were developed to study it. One of the most powerful and well established of these techniques is deep level transient spectroscopy (DLTS).[1] It is based on the variation of the capacitance of a Schottky junction as a measure of the number of charges trapped within its space charge region. DLTS provides important defects characteristics such as the defect concentration, energy level, thermal capture cross section, and emission cross sections. The behavior of the DLTS line amplitude as a function of the filling pulse time can provide additional information on the defect geometry, distinguishing pointlike from extended defects.

The standard DLTS procedure for a pointlike defect assumes that the capacitance transient associated to the electron emission obeys an exponential decay law. Therefore, multiply charged defects provide DLTS spectra that are difficult to correctly interpret. These difficulties arise from the many-step kinetic capture of these traps and of their nonexponential emissions. The problem becomes even more complicated if one of the defect charge state is metastable or strongly coupled to the lattice. Hence, large lattice relaxation (LLR) and thermal barriers for carrier capture have to be taken into account in any satisfactory description of spectra related to these deep level defects.

There are many reports in scientific literature of DLTS measurements of traps with two states of charge and which present strong coupling to the lattice. They were observed, for example, in Si,[2] InP,[4–6] CdTe,[7] $Hg_xCd_{1-x}Te$,[8,9] $Cd_xMn_{1-x}Te$,[10] GaAs,[13–16] GaSb,[17–21,23] $Al_xGa_{1-x}As$,[22,21] $Ga_xAs_{1-x}P$,[24] and $Zn_xCd_{1-x}Te$.[25] Most of them present an incomplete interpretation of their DLTS results due to the incompleteness of the model used.

It is the purpose of this paper to analyze the behavior of such defects under DLTS measurement conditions, discussing the reported experimental results in view of a model we have previously proposed.[9] The model is found to provide a general description of the spectra related to defects with two charge states and it permits one to understand some characteristics of this spectra that remained open, or not reasonably explained in the literature.

In Sec. II, we present a review of the model. We derive expressions for the occupation fraction of the defect at each of both charge states. A detailed discussion of the consequences of these expressions to the DLTS spectra is given. Finally, we show that the total DLTS signal originates from three different emission processes. In Sec. III, we classify and exemplify the deep levels according to the relative predominance of one of those three processes. With the help of computer simulation, reported DLTS spectra are reproduced, demonstrating good agreement between theoretically predicted and experimentally determined spectra. The work is summarized in Sec. IV.

## II. MODEL

In a previous paper,[9] we presented a model to describe the DLTS line behavior of a defect that can capture and emit two electrons. It was applied to explaining the unusual dependence of the DLTS line amplitudes with the filling pulse length observed in $Hg_{0.3}Cd_{0.7}Te$ submitted to ion implantation. The model assumes that each charge state of the defect appears as a distinct configuration in a DLTS measurement, in the sense that these states of charge have their own capture cross sections and activation energies. We are not concerned about how these parameters change after an electron capture but only with the fact that they are not a function of the trap occupation fraction. This last assumption precisely characterizes the trap as a pointlike defect.[26]

In a DLTS measurement, the traps are filled during a pulse time $t_p$ and emptied during a relaxation time $t_i$. These processes occur alternately at a frequency $f=(t_p+t_i)^{-1}$ when forward or reverse bias are applied to the Schottky contact.

During the filling period of duration $t_p$ (indicated by I), the trap can capture one or two electrons according to the reactions

 

$$D^{(n)}+e^- \xrightarrow{c_A} D^{(n-1)},$$

$$D^{(n)}+2e^- \xrightarrow{c_A} D^{(n-1)}+e^- \xrightarrow{c_B} D^{(n-2)}$$

in which $c_A$ and $c_B$ are the capture rates for the first and the second electrons, respectively.

We shall henceforth call the state of charge $D^{(n-1)}$ state $A$ and the state of charge $D^{(n-2)}$ state $B$.

The capture rate is related to the capture cross section $\sigma$ of the defect, the density of free electrons $n$, and their mean thermal velocity $\langle v^{\text{th}}\rangle$ by the equation

$$c_n=\sigma n\langle v^{\text{th}}\rangle. \tag{1}$$

We assume that the emission rates are very small compared with the capture rates during the filling period. Hence, from the detailed balance principle, the occupation fractions of defects in states $A$ and $B$ are given by the system of differential equations

$$\frac{\partial f_A^{\text{I}}}{\partial t}=c_A(1-f_A^{\text{I}}-f_B^{\text{I}})-c_B f_A^{\text{I}},$$

$$\frac{\partial f_B^{\text{I}}}{\partial t}=c_B f_A^{\text{I}}. \tag{2}$$

During the relaxation period of duration $t_i$ (indicated by II), the defect can emit a single electron according to the reactions

$$D^{(n-1)} \xrightarrow{e_A} D^{(n)}+e^-,$$

$$D^{(n-2)} \xrightarrow{e_B} D^{(n-1)}+e^-,$$

or a pair of electrons according to the reaction

$$D^{(n-2)} \xrightarrow{e_B} D^{(n-1)}+e^- \xrightarrow{e_A} D^{(n)}+2e^-,$$

in which $e_B$ and $e_A$ are the emission rates for the first and the second electrons, respectively.

The emission rates of the two charge states are given by the well-known relationship

$$e_n=\sigma_{\text{ap}}N_c\langle v^{\text{th}}\rangle\exp\left(-\frac{E_T}{kT}\right), \tag{3}$$

in which $\sigma_{\text{ap}}$ is the apparent capture cross section, $N_c$ is the effective density of states in the conduction band, and $E_T$ is the thermal activation energy necessary to emit an electron.

Due to the electric field, the capture rates are very small compared with the emission rates during the relaxation period. Thus, again from the detailed balance principle, the temporal evolution of the occupation fractions of defects in states $A$ and $B$ are given by the following system of differential equations:

$$\frac{\partial f_A^{\text{II}}}{\partial t}=-e_A f_A^{\text{II}}+e_B f_B^{\text{II}},$$

$$\frac{\partial f_B^{\text{II}}}{\partial t}=-e_B f_B^{\text{II}}. \tag{4}$$

If the rates of change of the defect charge state are fast compared with the heating rate of the sample, the steady state is attained and the occupation fractions at the end of the relaxation period are equal to the occupation fractions at the beginning of the filling period, and vice versa. Thus,

$$f_A^{\text{II}}|_{t_i=0}=f_A^{\text{I}}|_{t=t_p},$$

$$f_B^{\text{II}}|_{t_i=0}=f_B^{\text{I}}|_{t=t_p} \tag{5}$$

and

$$f_A^{\text{I}}|_{t_p=0}=f_A^{\text{II}}|_{t=t_i},$$

$$f_B^{\text{I}}|_{t_p=0}=f_B^{\text{II}}|_{t=t_i}. \tag{6}$$

Using the above steady-state conditions, we obtain the explicit expressions for the temporal evolution of the defect occupation fractions in both periods: (i) in period I ($0\leqslant t\leqslant t_p$),

$$f_A^{\text{I}}(t)=\left(\frac{c_1b_2-c_2b_1}{a_1b_2-a_2b_1}\right)e^{-c_Bt}+\frac{c_A}{c_B}\left(\frac{a_1c_2-a_2c_1}{a_1b_2-a_2b_1}\right)e^{-c_At}, \tag{7}$$

$$f_B^{\text{I}}(t)=1-\left(\frac{c_1b_2-c_2b_1}{a_1b_2-a_2b_1}\right)e^{-c_Bt}-\left(\frac{a_1c_2-a_2c_1}{a_1b_2-a_2b_1}\right)e^{-c_At}; \tag{8}$$

(ii) in period II ($0\leqslant t\leqslant t_i$),

$$f_A^{\text{II}}(t)=f_A^{\text{I}}(t_p)e^{-e_At}+\frac{e_B}{e_A-e_B}f_B^{\text{I}}(t_p)[e^{-e_Bt}-e^{-e_At}], \tag{9}$$

$$f_B^{\text{II}}(t)=f_B^{\text{I}}(t_p)e^{-e_Bt}. \tag{10}$$

The parameters $a_1$, $a_2$, $b_1$, $b_2$, $c_1$, and $c_2$ in Eqs. (7) and (8) are given by

$$a_1=1-e^{-e_Bt_i-c_Bt_p}, \tag{11}$$

$$b_1=1-e^{-e_Bt_i-c_At_p}, \tag{12}$$

$$c_1=1-e^{-e_Bt_i}, \tag{13}$$

$$a_2=1-e^{-e_At_i-c_Bt_p}+\frac{e_B}{e_A-e_B}[e^{-e_Bt_i}-e^{-e_At_i}]e^{-c_Bt_p}, \tag{14}$$

$$b_2=\frac{c_A}{c_B}[1-e^{-e_At_i-c_At_p}]+\frac{e_B}{e_A-e_B}[e^{-e_Bt_i}-e^{-e_At_i}]e^{-c_At_p}, \tag{15}$$

$$c_2=\frac{e_B}{e_A-e_B}[e^{-e_Bt_i}-e^{-e_At_i}]. \tag{16}$$

The unusual dependence between DLTS line amplitude and filling pulse length observed in defects that can capture two carriers (cf. Ref. 9 and Sec. III A) is one of many interesting consequences of the present model. In Secs. III A–III C we show that the model also predicts a dependence on line position with pulse time $t_p$ and a possible modification in its usual exponentially derived shapes. In addition, some DLTS spectra that could be misinterpreted as arising from an ordinary single charged pointlike defect will be simulated in Sec. III.

The rest of this section is devoted to obtaining from Eqs. (9) and (10) the mathematical expressions for the DLTS signal corresponding to the change of the occupation fractions in the relaxation period.

Equations (9) and (10) give, respectively, the fraction of defects in states $A$ and $B$ at time $t$ in the relaxation period. The first term on the right-hand side of Eq. (9),

$$f_A(t)=f_A^{\mathrm{I}}(t_p)e^{-e_A t}, \tag{17}$$

is the fraction of traps that were in state $A$ at the end of the filling period and that are still in state $A$ at time $t$.

The second term is the fraction of defects that were in state $B$ at the end of the filling period, but after the emission of one electron they are in state $A$ at time $t$. This term is the accumulation in $A$ during the relaxation period and is given by

$$A_c(t)=\frac{e_B}{e_A-e_B}\,f_B^{\mathrm{I}}(t_p)[e^{-e_B t}-e^{-e_A t}]. \tag{18}$$

It will be shown in Sec. III that the kinetics of the accumulation $A_c(t)$ characterizes the DLTS spectra of defects with two charge states. Hence, some attention to its behavior during the relaxation period is needed.

The function $A_c(t)$ increases from zero up to the maximum value

$$A_{c\ \max}=f_B^{\mathrm{I}}(t_p)\left(\frac{e_B}{e_A}\right)^{e_A/(e_A-e_B)} \tag{19}$$

at time

$$t_{\max}=\frac{1}{e_A-e_B}\ln\frac{e_A}{e_B} \tag{20}$$

and then it decreases to zero when $t\to\infty$. Its line shape has three kinetic regimes depending strongly on the ratio between the emission rates $e_A$ and $e_B$. The accumulation is small and slow when $e_A\gg e_B$ [Fig. 1(a)]; it is moderate [Fig. 1(b)] when $e_A\approx e_B$; and it is large and rapid when $e_A\ll e_B$ [Fig. 1(c)]. The three different types of DLTS spectra for defects with two charge states are a direct consequence of these three different kinetic regimes.

The fraction of traps that were in state $B$ at the end of the filling period and that are still in state $B$ or in state $A$ at time $t$ is expressed by

$$\begin{aligned} f_{AB}(t)&=f_B^{\mathrm{II}}(t)+A_c(t)\\ &=f_B^{\mathrm{I}}(t_p)\,\frac{e_A\exp(-e_B t)-e_B\exp(-e_A t)}{e_A-e_B}. \end{aligned} \tag{21}$$

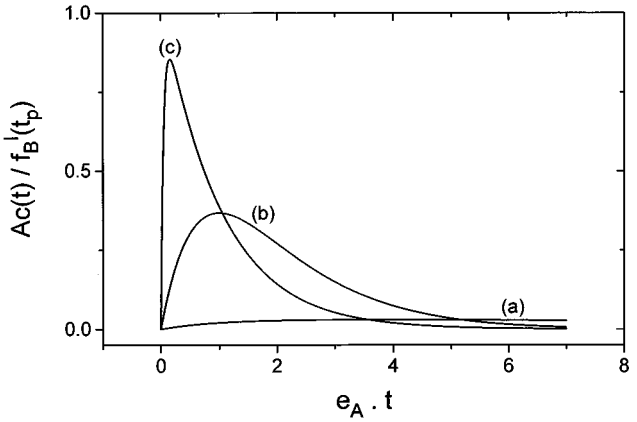


FIG. 1. Accumulation in $A$ as a function of $e_A t$ in the period $0\leqslant t\leqslant t_i$: (a) small and slow accumulation for $e_A\gg e_B$, (b) moderate accumulation for $e_A\approx e_B$, and (c) large and rapid accumulation for $e_A\ll e_B$.

The meaning of the fraction $f_{AB}(t)$ is not straightforward: it corresponds to the number of defects that can emit an electron at time $t$ in accordance with the second stage of the reaction $D^{(n-2)}\xrightarrow{e_B}D^{(n-1)}+e^-\xrightarrow{e_A}D^{(n)}+2e^-$. It is a monotonically decreasing function of time whose derivative (with the minus sign) is equal to the number of electrons emitted per unit time according to the second part of the reaction. In contrast, the fraction $f_B^{\mathrm{II}}(t)$ of defects in state $B$ at time $t$, given by Eq. (10), corresponds to the number of defects that can emit an electron at time $t$ in accordance with the first stage of the reaction. In this sense, we shall talk about the first emitted electron and the second emitted electron.

DLTS measurements take advantage of the fact that the transient of capacitance $\Delta C$ is due to the variation of charge within the space charge region of a Schottky contact during the relaxation period. If the density of defects $N_d$ is small compared to the dopant concentration $N_0$, the capacitance transient $\Delta C(t)$ is related to the local transient of the occupation fraction $\Delta f(z,t)$ by[27]

$$\Delta C(t)=-\frac{C_0 N_d}{N_0 w_0^2}\int_0^\infty \Delta f(z,t)z\,dz \tag{22}$$

($C_0$ is the capacitance and $w_0$ is the width of the space-charge region).

From Eq. (22) it is apparent that a capacitance transient is created whenever a lot of defects emit a charge carrier. Accordingly, the three emission processes by a trap with two charge states give rise to three different capacitance transients: (i) $\Delta C_A(t)$, related to the change of the occupation fraction $f_A(t)$ due to the exponential emission of a single electron; (ii) $\Delta C_B(t)$, related to the change of the occupation fraction $f_B^{\mathrm{II}}(t)$ due to the exponential emission of the first of a pair electrons; and (iii) $\Delta C_{AB}(t)$, related to the change of fraction $f_{AB}(t)$ due to the nonexponential emission of the second electron.

As the function $f_{AB}(t)$ decreases monotonically with time, its corresponding capacitance transient $\Delta C_{AB}(t)$ is always positive as would be expected for a majority carrier trap (cf. Ref. 1). We emphasize that if we had taken into

account for the calculation of $\Delta C_{AB}(t)$ only the accumulation fraction $A_c(t)$, we would have obtained a physically meaningless expression. This is due to the fact that $A_c(t)$ is not a monotonic function of $t$ (see Fig. 1) and its derivative is not equal to the number of electrons emitted in the second part of the reaction $D^{(n-2)} \xrightarrow{e_B} D^{(n-1)} + e^- \xrightarrow{e_A} D^{(n)} + 2e^-$.

The DLTS signal $L$ results from the convolution of the total capacitance transient $\Delta C(t) = \Delta C_A(t) + \Delta C_B(t) + \Delta C_{AB}(t)$ and is, therefore, the sum of the three corresponding signals $L_A$, $L_B$, and $L_{AB}$, given by

$$L_A = f_A^{\mathrm{I}}(t_p) r_A , \tag{23}$$

$$L_B = f_B^{\mathrm{I}}(t_p) r_B , \tag{24}$$

$$L_{AB} = f_B^{\mathrm{I}}(t_p) \frac{e_A r_B - e_B r_A}{e_A - e_B} , \tag{25}$$

in which $r_A$ and $r_B$ are the DLTS line amplitudes for an exponential emission at the rates $e_A$ and $e_B$. The normalized amplitudes $r_A$ and $r_B$, registered using the lock-in technique with square wave correlation at frequency $f = 1/(t_p + t_i)$, are given by

$$r_{A,B} = \frac{1}{0.204} \frac{f}{e_{A,B}} \left[ 1 - \exp\left( - \frac{e_{A,B}}{2f} \right) \right]^2 . \tag{26}$$

The signal $L_A$ arises from the exponential emission of an electron by traps that captured a single electron and the signals $L_B$ and $L_{AB}$ arise, respectively, from the exponential emission of a first electron and the nonexponential emission of a second electron by traps that captured two electrons.

Usually the DLTS signal for ordinary pointlike defects is characterized by an exponential emission rate. Since two emission rates $e_A$ and $e_B$ appear in the expression (25) for the signal $L_{AB}$, it is clear that this signal plays a key role in somewhat singular aspects presented by the DLTS spectra of defects with two charge states. Actually, line $L_{AB}$ is of a nonexponential type and it is not normalized by the factor 1/0.204 occurring in Eq. (26). Moreover, $L_{AB}$ is a kind of resultant signal from all processes involved in a second electron emission.

It should be noted that what is actually measured in an experiment is the total convolution signal $L$. As will be discussed in the next section, this fact can give rise to wrong interpretations of the experimental results.

## III. APPLICATION AND DISCUSSION

The above model characterizes the three possible types of DLTS spectra for a doubly charged defect according to the ratio of the emission rates of states $A$ and $B$. Each type of spectrum will be separately analyzed in the following subsections.

### A. Case $e_A \gg e_B$ applied to $p$-type CdTe

The first type of spectrum described by the model appears when $e_A \gg e_B$. Since the temperature $T_A$ at the maximum value of the signal $L_A$ is smaller than the temperature $T_B$ at the maximum value of the signal $L_B$, we shall call this type of spectrum the $AB$ spectrum.

Instances of the $AB$ spectrum were observed in Fe-doped InP (in the configuration $A$ of the so-called MFe center),[6] in $p$-type CdTe,[7] and in $n$-type $Hg_{0.3}Cd_{0.7}Te$.[8,9] Recently, a candidate for an $AB$ trap was also observed in $n$-type silicon after proton implantation.[28]

We shall apply our model to the particularly clear instance of a defect with the $AB$ spectrum observed by Zoth and Schröter[7] in $p$-type CdTe. They found two DLTS lines, labeled $H4$-$A$ and $H4$-$B$, manifesting unusual dependence on the filling pulse length $t_p$: line $A$ decreases while line $B$ increases with increasing $t_p$. For short pulses, line $A$ is observed with its maximum amplitude. For long pulses, line $A$ vanishes while line $B$ reaches it maximum amplitude, which is twice the maximum amplitude of line $A$.

Both lines are associated with the same defect, which can capture and emit two holes, line $H4$-$A$ corresponding to the emission of a single hole and line $H4$-$B$ corresponding to the simultaneous emissions of a pair of holes. The capture of the second hole is related to a large lattice relaxation and is thermally activated to such an extent that an inverted ordering of the emission energies is observed. From the electric field dependence of the hole emission rates, the authors were able to infer a donor character for a level and an acceptor character for the other, with positive-$U$ ordering. They attributed the defect to a Cd-vacancy complex.

In Fig. 2(a) we simulate a series of DLTS spectra for the defect as a function of the filling pulse length $t_p$. The essential features of the measured spectra shown in Fig. 2(a) of Ref. 7 are reproduced by the simulations. Figure 2(b) shows the total convolution signal $L$ and its components $L_A$, $L_B$, and $L_{AB}$ for the pulse length $t_p = 5$ $\mu$s.

The behavior of the observed lines is a consequence of the slow and small accumulation in state $A$ [see Fig. 1(a)]. Since $e_A \gg e_B$, the emission of the second hole follows immediately after the emission of the first hole and the accumulation $A_c(t)$ is very small in comparison with the fraction $f_B^{\mathrm{I}}(t_p)$. It results from Eqs. (23)–(25) that the signal $L_{AB}$ almost equals the signal $L_B$, $L_{AB} \approx f_B^{\mathrm{I}}(t_p) r_B = L_B$, and the total signal $L$ is approximately given by

$$L \approx f_A^{\mathrm{I}}(t_p) r_A + 2 f_B^{\mathrm{I}}(t_p) r_B . \tag{27}$$

Therefore, the maximum amplitude of the DLTS signal at temperature $T_B$ is twice the maximum amplitude at temperature $T_A$ [see Fig. 2(a)]. This result confirms the *ad hoc* expedient of doubling the fraction $f_B^{\mathrm{I}}(t_p)$ used in Refs. 6, 7, and 9.

We note that although the effect of the accumulation in $A$ is very small, it is not negligible at temperatures close to $T_A$. Figure 2(b) shows that the signals $L_{AB}$ and $L_B$ do not coincide at these temperatures, the difference being responsible for the deviations between the experimental data and calculations of Ref. 7.

Figure 3 shows the ratio of the total signal $L$ at temperatures $T_A$ and $T_B$ as a function of the filling pulse $t_p$ according to Eqs. (23)–(25) and the data points derived from Fig. 2(a) of Ref. 7. Theory and experience agree fairly well without any additional considerations about the slow capture in the so-called Debye tail.[27]

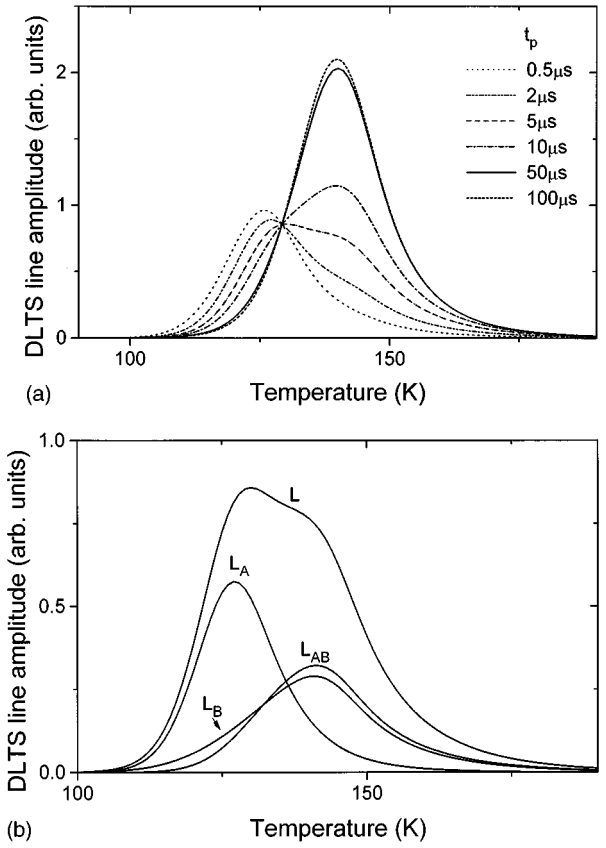


FIG. 2. (a) Computer-simulated DLTS spectra for the defects measured in $p$-type CdTe at a lock-in rate window of 712 $s^{-1}$. The simulation parameters were taken from Ref. 7 [$n$ (free-hole density)$\approx 10^{15}$ $cm^{-3}$, $\sigma_p(A)=5\times10^{-16}$ $cm^2$, $\sigma_p(B)=1.7\times10^{-16}$ $\exp(-0.07\ eV/kT)$]. The emission rates may be written as $e_p=AT^2\exp(-E_T/kT)$. The prefactor $A$ of $e_p$ is $5.1\times10^6$ $s^{-1}K^{-2}$ for state $A$ and $7.4\times10^6$ $s^{-1}K^{-2}$ for state $B$, respectively. The activation energy $E_T$ was 0.20 eV for state $A$ and 0.23 eV for state $B$. (b) Simulated spectra of (a) for $t_p=5$ $\mu$s showing the total convolution signal $L$ and its components $L_A$, $L_B$, and $L_{AB}$.

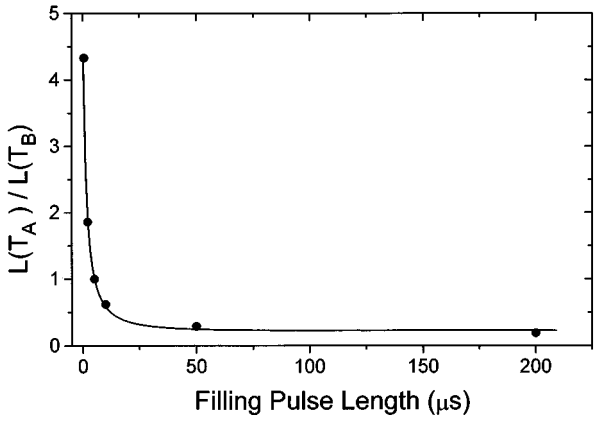


FIG. 3. Ratio between the total convolution signal $L$ at the temperature of the maximum value of signal $L_A(T_A)$ and the maximum value of signal $L_B(T_B)$ as a function of the filling pulse $t_p$. The circles represent this ratio as taken from the measured spectra [Fig. 2(a) of Ref. 7] whereas the solid line is the theoretically calculated one. Simulation parameters are the same as in Fig. 2(a).

### B. Case $e_A \ll e_B$ applied to $V_{As}$ in GaAs and $Cd_{1-x}Mn_xTe$:Ga

The second type of spectrum described by the model appears when $e_A \ll e_B$. Since the maximum value of the signal $L_B$ occurs at a lower temperature than the maximum value of the signal $L_A$, we shall call this type of spectrum the $BA$ spectrum.

Remarkable examples of defects exhibiting the $BA$ spectrum are the configuration $B$ of the MFe center in InP:Fe,[6] the divacancy in electron irradiated silicon,[11,12] the isolated arsenic vacancy $V_{As}$ in GaAs,[13,14,16,22] and the Ga-related $DX$ center in $Cd_{1-x}Mn_xTe$.[10] We shall apply our model to reproduce the main features of the measured spectra for GaAs and $Cd_{1-x}Mn_xTe$.

The $V_{As}$ defect is created by electron,[22,13] $\alpha$ particle, and proton[14,16] irradiation in $n$-type GaAs. The irradiation-induced defect is responsible for two DLTS peaks, labeled $E1$ and $E2$, which have been respectively attributed to an acceptorlike charge state $(-/0)$ and a donorlike charge state $(0/+)$ of the vacancy.[15] DLTS measurements also detected two dominant emission peaks in Ga-doped $Cd_{0.97}Mn_{0.03}Te$,[10] also labeled $E1$ and $E2$, with thermal activation energies for electron emission of 0.25 and 0.43 eV. The capture process of the $E1$ level is thermally activated, with a thermal energy barrier of 0.11 eV.

In both materials, the peaks $E1$ and $E2$ were found to obey a similar capture kinetics. The capture rate of the line $E1$ is very slow and can be determined with great accuracy, but the capture rate of line $E2$ is very fast and cannot be measured with the usual DLTS technique. Line $E1$ has been observed to increase with increasing $t_p$, while line $E2$ has been found with its maximum amplitude even for the shortest filling pulse available experimentally. The height of peak $E1$ after saturation nearly equals the height of peak $E2$. This fact was interpreted in Refs. 13 and 10 as evidence for the assumption that the pair of peaks detected in GaAs and $Cd_{0.97}Mn_{0.03}Te$:Ga may be related with two states of charge of the same defect that have positive-$U$ ordering.

The main features of the observed spectra are consequences of the large and fast accumulation $A_c(t)$ [see Fig. 1(c)]. Since $e_A \ll e_B$, almost all defects occupied by two electrons emit the first electron before time $t_{max}$ and the second electron after $t_{max}$. So, two peaks of nearly equal amplitudes are observed at temperatures $T_A$ and $T_B$. It results from Eqs. (23)–(25) that $L_{AB}\approx f_B^I(t_p)r_A$ and the total signal $L$ is approximately given by

$$L \approx f_B^I(t_p)r_b + [f_A^I(t_p) + f_B^I(t_p)]r_a . \tag{28}$$

Consequently, the DLTS signal at $T_A$ increases faster than the DLTS signal at $T_B$ with increasing pulse length $t_p$ and the signals have almost equal magnitudes after saturation, when $f_B^I(t_p)\approx 1$ and $f_A^I(t_p)\approx 0$.

In Fig. 4 we simulate the $BA$ spectrum for the isolated vacancy $V_{As}$ in GaAs under saturation conditions using the measured parameters of Ref. 14. In Fig. 5(a), we simulate two $BA$ spectra for the defect observed in $Cd_{0.97}Mn_{0.03}Te$ at $t_p=10$ $\mu$s (dashed line) and $t_p=1000$ $\mu$s (continuous line). Figure 5(b) shows the convolution signal $L$ and its components $L_A$, $L_B$, and $L_{AB}$ at $t_p=10$ $\mu$s. All the simulations are in good agreement with the observed DLTS spectra.

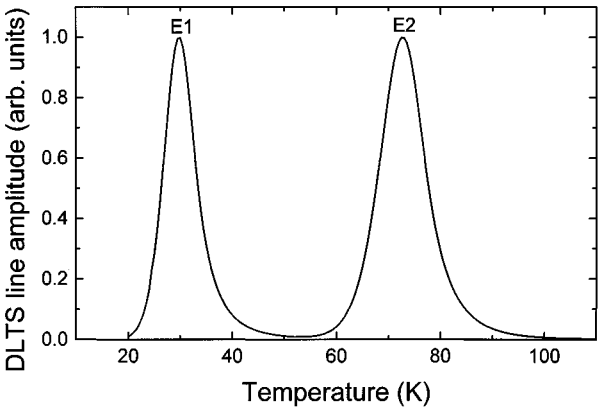


FIG. 4. Computer-simulated spectra for the isolated vacancy $V_{As}$ in $n$-type GaAs. The simulation parameters were derived from Ref. 14 [$t_p$=0.5 $\mu$s, lock-in frequency=46 Hz, $n$ (free electron density)=$1.2\times10^{16}$ cm$^{-3}$, $\sigma_n(A)=\sigma_{ap}(A)=1.5\times10^{-15}$ cm$^2$, $\sigma_n(B)=\sigma_{ap}(B)=1.3\times10^{-14}$ cm$^2$, $E_T(A)$=0.026 eV, and $E_T(B)$=0.117 eV].

### C. Case $e_A \approx e_B$ applied to the $DX$ center in GaSb:S

The third type of spectrum described by the model appears when $e_A \approx e_B$. As the temperatures $T_A$ and $T_B$ are very close to each other, one observes only a large, nonexponential peak. This type of spectrum will be called the $C$ spectrum.

An instance of the $C$ spectrum is exhibited by the sulfur related $DX$ center in GaSb.[20,19,18] The observed defect possesses similar properties to those of the $DX$ centers first detected in Te-doped $Al_xGa_{1-x}As$ (Ref. 22) and later in GaAs under high hydrostatic pressures[29] as well as with very high doping levels.[30,31] According to the model developed by Chadi and Chang,[32] the metastable phenomena characterizing the $DX$ center in III-V and II-VI semiconducting compounds arise from the interstitial-to-substitutional motion of the defect.[33] The $DX$ center is stabilized by the capture of two electrons and therefore has negative $U$,[2] its ground state being a negatively charged $D^-$ acceptor state. There is strong experimental evidence for the ground states of the Ge-related $DX$ center in GaAs, co-doped with Ge and Te,[34] and the sulfur-related $DX$ center in $GaAs_{1-x}P_x$ (Ref. 24) to possess a double electron occupation.

Dobaczewski and Kaczor[21] proposed a model for the negative-$U$ $DX$ center according to which the capture and emission processes between the ground state and the conduction band occur via an intermediate one-electron $D^0$ state by the reactions $D^- \leftrightarrow D^0 + e^- \leftrightarrow D^+ + 2e^-$. Observations of the temperature effect on the photoionization transients of the $DX$ center in $Al_xGa_{1-x}As$:Te and on the capacitance transients of the thermal emission process from the $DX$ center in GaSb:S were presented as experimental evidence for the existence of the intermediate $D^0$ state. From a system of rate equations similar to Eqs. (2) and (4), they derived expressions for the concentrations of defects possessing one or two electrons under the isothermal DLTS measurement conditions. Since the isothermal DLTS is the null frequency limit of the steady state DLTS (exposed in Sec. II), their expressions are particular cases of Eqs. (7)–(10), valid for large enough values of $t_i$ to empty all the defects ($t_i \to \infty$).

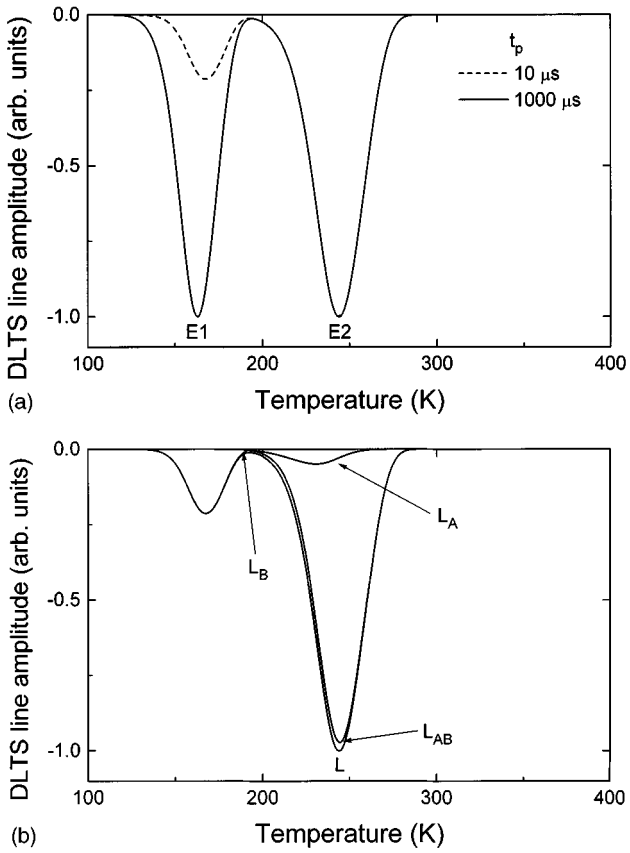


FIG. 5. (a) Computer-simulated DLTS spectra for Ga-doped $Cd_{0.97}Mn_{0.03}Te$. The simulation parameters were derived from Ref. 10 [double-boxcar rate window=$1.2\times10^3$ s$^{-1}$, $n=2\times10^{16}$ cm$^{-3}$, $\sigma_n(A)=\sigma_{ap}(A)=5\times10^{-14}$ cm$^2$, $\sigma_n(B)=1\times10^{-16}\exp(-0.11\ \text{eV}/kT)$ cm$^2$, $\sigma_{ap}(B)=7.7\times10^{-15}$ cm$^2$, $E_T(A)$=0.43 eV, and $E_T(B)$=0.25 eV]. (b) Simulated spectra of (a) for $t_p=10$ $\mu$s showing the total convolution signal $L$ and its components $L_A$, $L_B$, and $L_{AB}$.

Their model was applied for the case of the $DX$ center in GaSb:S. The values of the thermal emission and capture rates were obtained by fitting the observed capacitance transients to the sum of the concentrations of defects in both charge states, which are essentially given by Eqs. (9) and (10). This procedure is not correct since it ignores the contribution of the fraction of defects occupied by two electrons [$f_B^{II}(t)$] to the partial DLTS signal ($L_{AB}$) arising from the emission of the second electron (see Sec. II). The fitting of the DLTS line amplitudes for different filling pulses shown repeatedly in Refs. 17, 21, and 23 is therefore rather artificial.

As a matter of fact, the capture rate of the second electron is too fast to be observed, even for the shortest filling pulses, and the capture rate of the first electron is the rate-limiting step (see below). The fraction $f_A^I(t_p)$ is negligible and the fraction $f_B^I(t_p)$ is very accurately given by

$$f_B^I(t_p) \approx 1 - e^{-c_A t_p}. \tag{29}$$

So the states $D^+$ and $D^-$ are simultaneously present for short filling pulses, but not state $D^0$, which is a characteristic negative-$U$ property for a defect.[2] It results from Eqs. (23)–

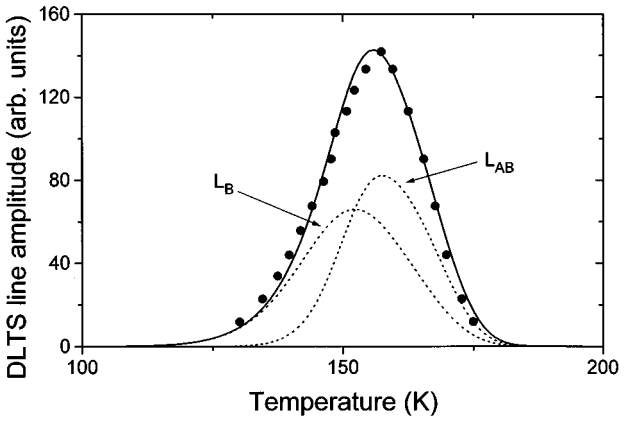


FIG. 6. Comparison of measured DLTS line (●) in $n$-type GaSb:S as taken from Fig. 1(a) of Ref. 20 ($t_p$=20 ms, double boxcar rate window=200 $s^{-1}$) with computer fitted line [$\sigma_{ap}(A)=5\times10^{-14}$ cm$^2$, $\sigma_{ap}(B)=9\times10^{-16}$ cm$^2$, $E_T(A)=0.27$ eV, and $E_T(B)=0.22$ eV].

(25) that only the signals $L_B$ and $L_{AB}$ contribute to the total convolution signal $L$, which is given by

$$L \approx f_B^{\mathrm{I}}(t_p)\left(r_B + \frac{e_A r_B - e_B r_A}{e_A - e_B}\right). \tag{30}$$

In Fig. 6 we adjust our model to data points drawn from the measured spectrum for GaSb:S that is shown in Fig. 1 of Ref. 20. The parameters adopted for the fitting are the emission activation energies $E_A$=0.27 eV, $E_B$=0.22 eV, and the apparent capture cross sections $\sigma_A=5\times10^{-14}$ cm$^2$, $\sigma_B=9\times10^{-16}$ cm$^2$. These values are not far from those reported in Refs. 18–20. We emphasize that only the partial signals $L_B$ and $L_{AB}$ (dotted lines) contribute to the total convolution signal. Our simulations reveal that this is also true for short filling pulses, when the line amplitude is not yet saturated.

## IV. CONCLUSION

We developed a model to account for the DLTS line behavior of defects possessing two charge states. Applying the model to reported measurements, we described the main features of the three possible types of spectra, called $AB$, $BA$, and $C$. The main characteristic of the $AB$ spectrum is the unusual dependence of line amplitudes with filling pulse length. Line $A$ decreases whereas line $B$ increases with increasing $t_p$. This has been observed in Fe-doped InP, $p$-type CdTe, and $Hg_{0.3}Cd_{0.7}Te$ submitted to ion implantation. The $BA$ spectrum has been found in radiation-damaged $n$-type GaAs, Fe-doped InP, electron irradiated silicon, and heavily Ga-doped $Cd_{0.97}Mn_{0.03}Te$ for defects having positive-$U$ correlation energy. It is characterized by the presence of two peaks with almost the same amplitude after saturation. Finally, the main feature of the $C$ spectrum is the detection of a single broadened peak. It has been measured in sulfur-doped GaSb and it is related to a negative-$U$ $DX$ center. The simulations agree qualitatively as well as quantitatively with experience and show the applicability of the model to positive-$U$ and negative-$U$ systems.

## ACKNOWLEDGMENTS

The authors would like to thank Professor C. J. F. Graff and Professor P. Vercelli for suggestions concerning this paper. This work was partially supported by the CNPq, CAPES, and PADCT.

*Present address: Instituto de Física Gleb Wataghin, UNICAMP, Caixa Postal 6165, 13081, Campinas, SP, Brazil.

[1] D. V. Lang J. Appl. Phys. **45**, 3023 (1974).
[2] R. D. Harris, J. L. Newton, and G. D. Watkins, Phys. Rev. Lett. **48**, 1271 (1982).
[3] G. D. Watkins, *Festkörperprobleme: Advances in Solid State Physics*, edited by P. Grosse (Vieweg-Verlag, Braunschweig, 1984), Vol. 24, p. 163.
[4] M. Levinson, J. L. Benton, and L. C. Kimerling, Phys. Rev. B **27**, 6216 (1983).
[5] M. Levinson, M. Stavola, J. L. Benton, and L. C. Kimerling, Phys. Rev. B **28**, 5848 (1983).
[6] M. Levinson, M. Stavola, P. Besoni, and W. A. Bonner, Phys. Rev. B **30**, 5817 (1984).
[7] G. Zoth and W. Schröter, Philos. Mag. **58**, 623 (1988).
[8] J. F. Barbot, P. Girault, C. Blanchard, and I. A. Hümmelgen, J. Mater. Sci. **30**, 3471 (1995).
[9] M. Koehler, E. F. Ferrari, J. F. Barbot, and I. A. Hümmelgen, Phys. Rev. B **53**, 7805 (1996).
[10] N. G. Semaltianos, G. Karczewsky, B. Hu, T. Wojtowicz, and J. K. Furdyna, Phys. Rev. B **51**, 17 499 (1995).
[11] B. G. Svensson and M. Willander, J. Appl. Phys. **62**, 2758 (1987).
[12] J. Lalita, C. Jagadish, and B. G. Svensson, Nucl. Instrum. Methods Phys. Res. Sect. B **106**, 234 (1995).
[13] D. Pons and J. C. Bourgoin, J. Phys. C **18**, 3839 (1985).
[14] S. A. Goodman, F. D. Auret, and W. E. Meyer, Nucl. Instrum. Methods Phys. Res. Sect. B **90**, 349 (1990).
[15] B. Ziebro, J. H. Hemsky, and D. C. Look, J. Appl. Phys. **72**, 78 (1992).
[16] S. T. Lai, D. Alexiev, and B. D. Nener, J. Appl. Phys. **78**, 3686 (1995).
[17] L. Dobaczewski, P. Kaczor, G. Karczewsky, and I. Poole, Acta Phys. Pol. A **79**, 133 (1991).
[18] P. S. Dutta, K. S. R. Koteswara Rao, K. S. Sangunni, H. L. Bhat, and Vikram Kumar, Appl. Phys. Lett. **65**, 1412 (1994).
[19] P. Hubík, V. Smíd, J. Kristofik, B. Stepanek, and V. Sestakova, Solid State Commun. **86**, 19 (1993).
[20] I. Poole, M. E. Lee, I. R. Cleverley, A. R. Peaker, and K. E. Singer, Appl. Phys. Lett. **57**, 1645 (1990).
[21] L. Dobaczewski and P. Kaczor, Semicond. Sci. Technol. **6**, B51 (1991).
[22] D. V. Lang, R. A. Logan, and M. Jaros, Phys. Rev. B **19**, 1015 (1979).
[23] L. Dobaczewsky and P. Kaczor, Semicond. Sci. Technol. **6**, B51 (1991); Mod. Phys. Lett. B **6**, 15 (1992).
[24] M. F. Li, Y. Y. Luo, P. Y. Yu, E. R. Weber, H. Fujioka, A. Y. Du, S. J. Chua, and Y. T. Lim, Phys. Rev. B **50**, 7996 (1994).
[25] K. Khachaturyan, M. Kaminska, E. R. Weber, P. Becla, and R. A. Street, Phys. Rev. B **40**, 6304 (1989).
[26] W. Schröter, J. Kronewitz, U. Gnauert, F. Riedel, and M. Seibt,

Phys. Rev. B **52**, 13 726 (1995).
[27] D. Pons, J. Appl. Phys. **55**, 3644 (1984).
[28] J. F. Barbot, C. Blanchard, E. Ntsoenzok, and J. Vernois, Mat. Sci. Eng. B **36**, 81 (1996).
[29] M. Tachikawa, M. Mizuta, H. Kukimoto, and S. Minomura, Jpn. J. Appl. Phys. **24**, L821 (1985).
[30] D. K. Maude, J. C. Portal, I. D. Mowski, T. Foster, L. Eaves, M. Nathan, M. Heilbum, J. J. Haris, and R. B. Beal, Phys. Rev. Lett. **59**, 815 (1988).
[31] T. N. Theis, P. M. Mooney, and S. L. Wright, Phys. Rev. Lett. **60**, 361 (1988).
[32] D. J. Chadi and K. J. Chang, Phys. Rev. B **39**, 10 063 (1989).
[33] D. A. W. Soares, G. M. Ribeiro, J. F. Sampaio, A. S. Chaves, and A. G. Oliveira, Brazilian J. Phys. **24**, 370 (1994).
[34] M. Baj, L. H. Dmowski, and T. Slupiński, Phys. Rev. Lett. **71**, 3529 (1993).